Geophys. J. R. astr. Soc. (1983) **73**, 367–387

Palaeomagnetism of the Proterozoic Zig-Zag Dal Basalt and the Midsommersø Dolerites, eastern North Greenland

Christian Marcussen* and Niels Abrahamsen

Laboratory of Geophysics, University of Århus, Finlandsgade 8, DK-8200 Århus N, Denmark

Received 1982 October 14; in original form 1982 June 4

Summary. Palaeomagnetic investigations are reported from 24 sites in the Proterozoic Zig-Zag Dal Basalt Formation and 12 sites in the Midsommersø Dolerites of eastern North Greenland. The Zig-Zag Dal Basalt is a typical tholeiitic flood basalt sequence, and dolerite intrusions in the underlying sandstones are thought to be genetically related to the basalts.

After a detailed AF demagnetization programme 19 sites in the basalts and 10 sites in the dolerites reveal one stable component of magnetization, probably of TRM and/or CRM origin residing in small single domain titanomagnetite grains. The degree of anisotropy has not affected the direction of the remanent magnetization. The maximum axis of the anisotropy ellipsoid is parallel to the flow direction of the magma, whereas the minimum axis is perpendicular to the flow plane.

Only one polarity of the geomagnetic field was found. The mean palaeomagnetic pole positions for the two rock types are not significantly different (basalt: 12.2°S, 62.8°E with $A_{95} = 3.8°$; dolerites: 6.9°S, 62.0°E with $A_{95} = 5.1°$). After correction for Phanerozoic drift of Greenland the two mean poles compare closely to a relevant North American APW-curve for 1250–1350 Ma, in good agreement with Rb-Sr isochron ages of 1250 Ma obtained for the intrusives. The palaeogeographical position of Greenland was near equator with the major geographical axis orientated E–W.

1 Introduction

The late Proterozoic Zig-Zag Dal Basalt Formation of eastern North Greenland belongs to the oldest known tholeiitic flood basalts largely unaffected by later deformation and metamorphism (Kalsbeek & Jepsen 1983). The underlying sandstones of the Independence Fjord Group are intruded by numerous dolerite sills and dykes, which are thought to be genetically related to the basalts (Jepsen & Kalsbeek 1979).

*Present address: The Geological Survey of Greenland, Øster Voldgade 10, DK-1350 Copenhagen, K, Denmark.

The investigated palaeomagnetic samples from the basalts and dolerites form a part of a large collection of orientated rock samples collected during the Geological Survey of Greenland (GGU) expeditions to North Greenland in the summers of 1979 and 1980 (Henriksen 1981). This paper summarizes the results of palaeomagnetic and rock magnetic investigations of the two rock types. Preliminary results have previously been reported (Abrahamsen & Marcussen 1980; Marcussen 1981).

2 Geology and age

The platform area of eastern North Greenland contains a more than 8000 m thick sequence of flat-lying late Proterozoic to lower Palaeozoic sediments (Henriksen 1981). A crystalline basement, in this area of Greenland hidden below the Inland Ice, is overlain by a thick sequence of late Proterozoic continental sandstones, the Independence Fjord Group (Collinson 1980). These in turn are conformably overlain by the Zig-Zag Dal Basalt Formation (Jepsen & Kalsbeek 1979; Jepsen, Kalsbeek & Suthern 1980; Kalsbeek & Jepsen 1983). The basalts are unconformably overlain by sandstones of the upper Proterozoic Campanuladal Formation (Clemmensen 1979).

The basalts are located in central Mylius-Erichsen Land (Fig. 1) and in the eastern part of J. C. Christensen Land. The exposed area now covers an area of about 10 000 km^2, but it is most likely that the basalts originally occupied a much larger area. The thickness varies between *c.* 100 m at the northern and southern borders of the outcrop area and a maximum of *c.* 1350 m at the type section in Zig-Zag Dal (Fig. 2, Jepsen *et al.* 1980). The formation is divided into three major units in ascending order: the Basal Unit, the Aphyric Unit and the Porphyritic Unit.

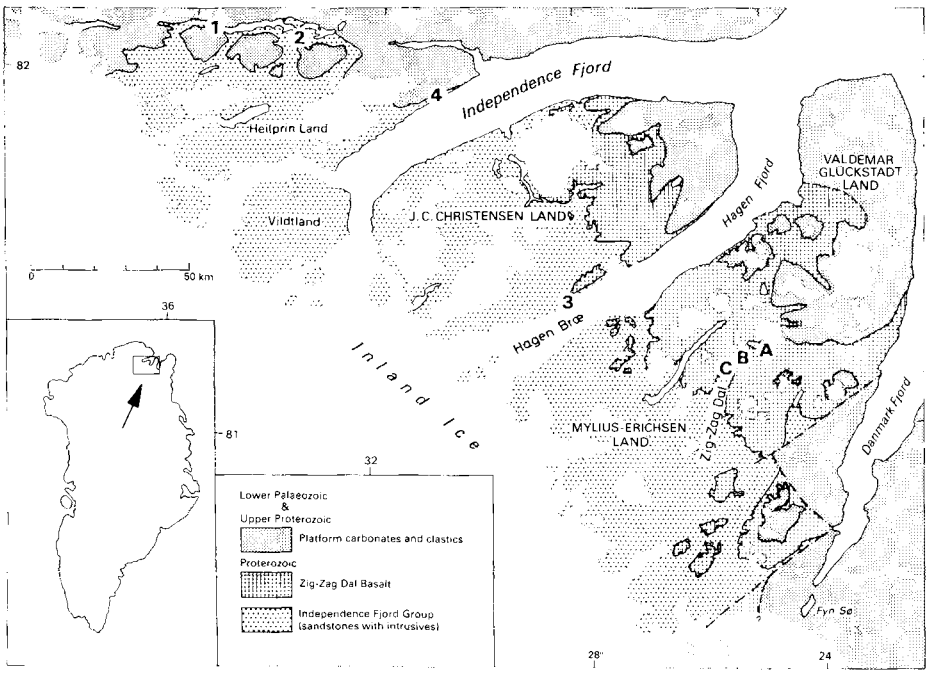

Figure 1. Geological map showing the main area of the Proterozoic Zig-Zag Dal Basalt and the sandstones of the Independence Fjord Group in the platform area of eastern North Greenland (from Jepsen *et al.* 1980). A, B and C denotes the sample sites in the type section of the basalts at Zig-Zag Dal. The numbers indicate the position of the dolerite localities.

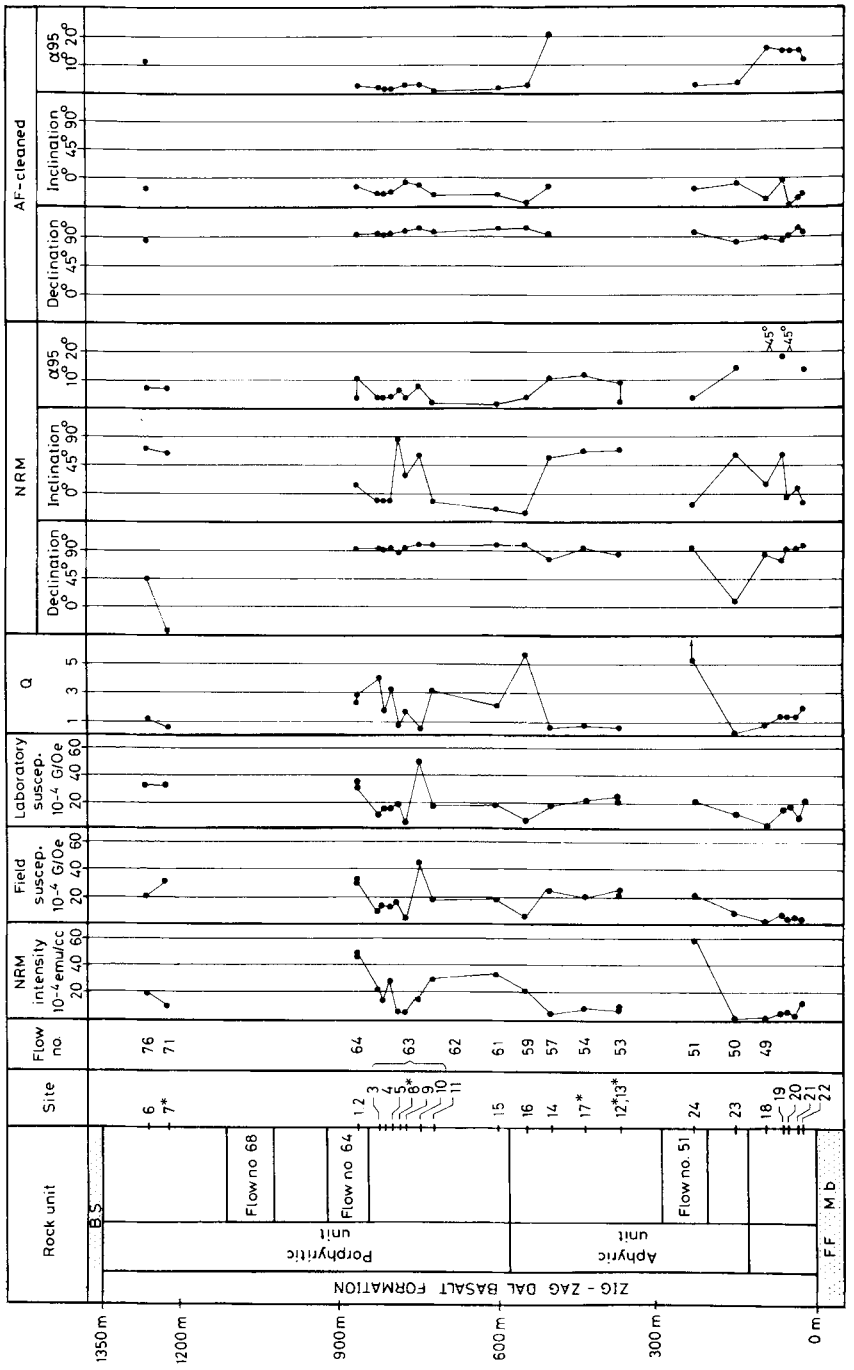

Figure 2. Geological profile of the basalt sequence in Zig-Zag Dal in Mylius-Erichsen Land (from Jepsen *et al.* 1980) with rock and palaeomagnetic mean data (*cf.* Tables 1a and 2a). FF Mb below the basalt is the Fiil Fjord Member of the Independence Fjord Group (Collinson 1980), whereas BS on top of the basalts is the basal sandstone association of the Campanuladal Formation (Clemmensen 1979). For reasons of clarity the site mean values have been connected. Unstable sites are marked with an asterisk.

The Basal Unit (100–120 m thick) is composed of small aphyric basalt flows, varying in thickness from less than 1 to 10 m. Pillow lavas, indicating subaqueous effusion, are found in the lower part of the unit. A thin (1–10 m) sediment horizon, consisting of sandstone and dolomite, overlies the Basal Unit at some places. The basalts in this unit are rather altered, which may be related to the subaqueous effusion of these flows (Kalsbeek & Jepsen 1983).

The Aphyric Unit (390–440 m thick) and the Porphyritic Unit (up to 750 m thick) are together composed of about 30 flows, varying in thickness from 10 to 120 m. Some of the thicker flows with characteristic features can be recognized and traced through all measured sections (Jepsen *et al.* 1980). Most flows are of aa-type and have vesicular, amygdaloidal or flowbrecciated tops preserved. These essentially non-erosional tops probably indicate that there were only short time intervals between the deposition of the individual flows.

The basalt sequence occupies today a trough-shaped basin which has been peneplained at the top. After the termination of, and possibly during, the volcanic activity, the central part of the basalt area underwent subsidence, and subsequently the area was subjected to a long period of erosion. This erosion probably removed all of the basalt lying to the east and west of the present outcrop area, before the deposition of the overlying basal sandstone association of the Campanuladal Formation took place.

The sandstones of the underlying Independence Fjord Group are intruded by numerous large sills as well as steeply dipping sheets and dykes of dolerites, which have a quartz-tholeiitic composition (Jepsen 1971; Jepsen & Kalsbeek 1979). Sills are the most common intrusion type, varying in thickness up to several hundreds of metres.

The dolerites in the Jørgen Brønlund Fjord area (Fig. 1) are called Midsommersø Dolerites (Jepsen 1971). For convenience this name is used for all the sampled dolerites investigated in this paper.

Rb-Sr isotope studies on the clay minerals in a siltstone unit in the Independence Fjord Group (Larsen & Graff-Petersen 1980) suggest an age of deposition of approximately 1380 Ma. Attempts to date the overlying basalt by the Rb-Sr whole rock method were unsuccessful (Kalsbeek & Jepsen 1983). However, the intrusives of the Independence Fjord Group have yielded well-defined Rb-Sr isochron ages of *c.* 1250 Ma (Jepsen & Kalsbeek 1979; Jepsen *et al.* 1980). The stratigraphical positions of the basalts makes it likely that this age is also the age of eruption of the basalts.

3 Palaeomagnetic investigations

3.1 SAMPLING

Samples were collected either as drilled cores using a water cooled portable drill or as hand samples and the orientation was always performed using a sun compass. A total of 198 samples was collected from 24 sites in the basalt sequence at Zig-Zag Dal (Figs 1 and 2), so as to include at least eight samples from each site, with the exception of the five sites in the Basal Unit, where only three or four hand samples were collected in each case.

The dolerite samples representing four different localities were collected from 12 sites (Fig. 1). The first six sites (DL01–06) were on a major sill (about 100 m thick) situated west of Øvre Midsommersø (locality 1), DL-07 on a sill between Øvre and Nedre Midsommersø (locality 2), DL-08 and 09 on dykes on the north side of Hagen Brae (locality 3) and DL10–12 on a sill (about 20–30 m thick) in Heilprin Land (locality 4). A total of 125 samples was collected, at least eight from each site.

In the laboratory several 1″ orientated cores were drilled from each hand sample and all cores were sliced into 2.3 cm long specimens. A total of 882 specimens in the basalts and 417 specimens in the dolerites were obtained.

The tectonic strike and dip of the lava flows and/or sediments (intruded by the dolerites) were measured in order to be able to carry out a bedding correction of the palaeomagnetic site mean directions (Table 2).

3.2 TECHNIQUES APPLIED

The NRM and anisotropy of the suceptibility were measured using two different Digico spinner magnetometers and the stability of the remanence was investigated in a detailed programme of stepwise AF demagnetization in zero field ($\pm 10\gamma$). The magnetic susceptibility was measured *in situ* and in the laboratory using low field bridge type instruments (Christie & Symons 1969). Susceptibility versus temperature was studied on powder samples in order to determine the Curie temperatures (Stephenson & de Sa 1970). Finally, polished sections of samples from 20 sites were examined under the ore microscope.

3.3 ROCK MAGNETIC RESULTS

In Fig. 2 (*cf.* Table 1) the mean value of the NRM intensity, susceptibility and NRM direction for the basalts are given in relation to the type section at Zig-Zag Dal. The NRMs of all specimens were measured and Fisher statistics (Fisher 1953) were used hierarchically (specimen, samples, sites) to obtain group mean directions. The within-sample scatter was generally very small for both rock types.

The sites in the Basal Unit show the lowest intensity and susceptibility values, probably due to alteration. The highest intensity value is found in the very prominent flow no. 51 (Fig. 2), whereas site BA-10 shows the highest susceptibility. No significant differences have been found in the rock magnetic parameters between the two upper units.

The two dolerite sites from locality 3 (at Hagen Brae) show high intensity and susceptibility values (Table 1). At locality 1 (except site DL-01) and at locality 4 we find intermediate values with little scatter.

The Q-values [Q = NRM/(lab. susc. $\times$ H), H = 0.555 G (measured *in situ*)] range between 0.3 and 10.2, probably indicating variable stability of the NRM. The Q-values are lowest for the dolerites due to their higher susceptibility.

The two sets of susceptibility data were obtained in different ways by two different instruments. The field measurements (15–20 readings, measuring volume *c.* 100 cm^3) were randomly distributed at each site, covering an area of about 10 m^2, whereas the laboratory measurements were made on about 15 specimens (volume *c.* 11 cm^3) from each site. The good agreement between the two data sets indicates magnetic homogeneity at the measured sites.

The anisotropy of the susceptibility was measured on one selected specimen from each sample. The degree of anisotropy ($A_n = \kappa_{max}/\kappa_{min}$) is listed in Table 1. The dolerites show fairly constant A_n-values of about 1.08. The Porphyritic Unit in the basalts has the highest A_n-value.

Less than half of all sites show well-defined directions of the axes of the anisotropy ellipsoid. The minimum axis is generally vertical for the basalt flows, whereas the dolerites show a more complicated pattern. In Fig. 3 two examples from sites with well-defined axes are plotted.

In Fig. 4 the site mean values of the NRM directions are plotted (*cf.* Table 1) for the two rock types. The inclination values are somewhat scattered, whereas the declination values generally trend towards the east. The mean directions appear to be smeared along a vertical great circle. Sites with high Q-values tend to have low or negative inclination values indicating little or no viscous components of NRM at these sites.

Table 1. (a) Zig-Zag Dal Basalt Formation, rock magnetic results.

Site	NRM	Confid. interval	Field susc.	Confid. interval	Lab. susc.	Confid. interval	Q	δ	A_n	N	D_m	I_m	k	α_{95}
	10^{-4}	emu/cm^3	10^{-4}	G/Oe	10^{-4}	G/Oe		g/cm^3			(°)	(°)		(°)
BA-01	47.8	43 - 53	32.1	30 - 35	36.3	35 - 38	2.38	2.90	1.15	9	91.8	9.3	216	3.5
BA-02	50.2	39 - 64	31.1	28 - 35	33.4	31 - 36	2.70	2.88	1.14	10	90.8	13.1	23	10.2
BA-03	23.6	20 - 29	10.9	8 - 15	10.8	8 - 14	3.95	2.75	1.09	9	93.9	-12.3	191	3.7
BA-04	14.4	11 - 19	14.2	10 - 21	14.5	10 - 20	1.78	2.84	1.06	8	90.7	-12.0	264	3.4
BA-05	28.7	18 - 45	14.1	12 - 16	15.5	14 - 17	3.33	2.85	1.05	10	92.9	-12.1	203	3.4
BA-06	19.2	16 - 23	21.0	18 - 24	32.6	28 - 38	1.06	2.89	1.15	9	44.7	71.5	45	7.7
BA-07	10.3	6 - 18	32.0	24 - 44	32.3	24 - 44	0.58	2.79	1.12	10	303.4	66.6	44	7.4
BA-08	6.7	5 - 9	16.2	12 - 22	17.4	13 - 23	0.70	2.90	1.06	9	87.0	83.1	77	5.8
BA-09	5.2	4 - 6	6.3	3 - 14	5.7	5 - 7	1.64	2.88	1.06	9	94.2	27.8	268	3.1
BA-10	16.3	12 - 22	45.8	42 - 50	50.6	46 - 56	0.58	2.92	1.05	9	101.8	70.8	43	7.9
BA-11	30.2	28 - 33	18.5	17 - 21	17.3	15 - 21	3.15	2.93	1.11	9	98.8	-14.8	866	1.7
BA-12	10.0	8 - 13	26.2	24 - 28	24.7	23 - 27	0.74	2.87	1.07	8	87.0	73.3	40	8.8
BA-13	8.3	7 - 9	22.7	21 - 24	22.7	20 - 26	0.67	2.86	1.09	9	84.6	78.1	478	2.3
BA-14	6.5	4 - 11	24.5	19 - 33	20.4	14 - 30	0.58	2.92	1.07	10	74.7	58.1	22	10.5
BA-15	34.1	30 - 38	18.8	16 - 22	19.9	18 - 22	3.08	2.93	1.10	10	99.3	-24.7	415	2.3
BA-16	21.8	17 - 28	7.6	6 - 10	7.0	6 - 9	5.60	2.86	1.07	10	99.6	-34.2	155	3.8
BA-17	9.2	8 - 11	21.2	19 - 24	21.1	19 - 21	0.79	2.88	1.07	9	93.0	71.0	21	11.5
BA-18	0.8	0.5-1.5	1.6	1 - 2	2.0	1 - 4	0.72	2.71	1.04	3	83.4	17.4	4	75.0
BA-19	6.0	5 - 7	9.3	8 - 11	7.8	7 - 9	1.39	2.75	1.04	4	76.9	60.2	26	18.2
BA-20	7.7	6 - 9	5.0	2 - 14	9.7	8 - 12	1.42	2.71	1.05	3	90.6	- 4.9	3	> 90
BA-21	4.0	3 - 6	6.5	5 - 9	5.3	4 - 8	1.37	2.70	1.07	3	91.7	9.5	8	47.6
BA-22	12.8	10 - 16	5.2	3 - 11	12.1	11 - 13	1.91	2.71	1.05	3	98.9	-12.7	84	13.5
BA-23	2.1	2 - 3	9.5	8 - 12	13.0	10 - 17	0.29	2.94	1.05	10	10.8	62.6	13	13.7
BA-24	119.5	79 -181	20.6	19 - 23	21.2	19 - 23	10.16	2.87	1.09	10	91.5	- 9.8	200	3.4
Porphyric	19.3	9 - 40	19.1	11 - 33	20.5	11 - 38	1.70	2.87	1.09	12	91.0	22.8	3	28.5
Aphyric	11.5	3 - 40	14.1	8 - 25	17.3	11 - 27	1.20	2.89	1.07	7	82.1	50.1	3	41.2
Basal unit	4.5	2 - 13	4.8	2 - 9	6.3	3 - 13	1.29	2.72	1.05	5	89.5	13.1	8	28.9
All	12.3	4 - 36	13.9	6 - 30	15.2	7 - 32	2.11	2.84	1.08	24	88.8	28.0	4	18.3
s(x)								0.08	0.03					

(b) Midsommersø Dolerites, rock magnetic results.

Site	NRM	Confid. interval	Field susc.	Confid. interval	Lab. susc.	Confid. interval	Q	δ	A_n	N	D_m	I_m	k	α_{95}
	10^{-4}	emu/cm^3	10^{-4}	G/Oe	10^{-4}	G/Oe		g/cm^3			(°)	(°)		(°)
DL-01	0.5	0.4-0.7	1.7	1 - 3	1.6	1 - 3	0.58	2.72	1.03	10	74.7	11.4	19	11.2
DL-02	9.6	8 - 12	22.8	16 - 32	25.3	21 - 30	0.68	2.77	1.15	13	75.7	37.9	27	8.0
DL-03	6.2	2 - 18	15.0	5 - 45	25.2	9 - 68	0.45	2.81	1.04	9	77.9	48.9	17	12.7
DL-04	15.2	13 - 18	28.2	26 - 30	28.7	26 - 31	0.97	2.81	1.12	10	75.6	17.3	82	5.3
DL-05	9.9	7 - 15	27.6	21 - 36	29.6	28 - 31	0.59	2.78	1.05	8	74.8	63.4	60	7.2
DL-06	13.0	12 - 14	29.4	27 - 33	31.2	30 - 33	0.76	2.78	1.11	9	82.5	30.3	83	5.6
DL-07	0.06	0.04-0.09	—	—	0.02	0.02-0.03	4.20	2.56	1.82	9	59.9	76.6	4	31.6
DL-08	81.8	54 -123	44.2	22 - 90	43.7	37 - 52	3.37	2.92	1.09	10	96.3	-35.4	95	4.9
DL-09	52.7	43 - 65	26.0	19 - 36	30.1	28 - 33	3.15	2.96	1.08	10	98.8	-29.3	476	2.2
DL-10	14.3	11 - 19	18.7	16 - 23	22.4	21 - 24	1.15	2.76	1.07	12	84.3	3.2	67	5.3
DL-11	13.5	12 - 15	14.6	12 - 18	18.3	15 - 23	1.33	2.74	1.10	12	88.7	10.5	42	6.7
DL-12	15.1	12 - 20	19.8	14 - 29	16.2	13 - 20	1.68	2.57	1.08	11	84.2	39.8	21	10.1
Loc.1	6.2	2 - 22	15.4	5 - 47	17.3	5 - 56	0.65	2.78	1.08	6	76.0	34.8	17	16.6
Loc.2	65.7	48 - 90	33.9	23 - 49	36.3	28 - 47	3.26	2.94	1.09	2	97.5	-32.5	315	14.1
Loc.3	14.3	14 - 15	17.6	15 - 21	18.8	16 - 22	1.37	2.69	1.08	3	85.8	17.7	17	30.5
All (-DL7)	12.0	3 - 44	18.4	8 - 43	20.3	8 - 49	1.34	2.77	1.08	11	82.9	23.6	6	19.8
s(x)								0.12	0.04					

Notes:
The NRM intensity, field susc. and lab. susc. figures tabulated are geometrical mean values. The confidence intervals have been calculated using the formula: $[\![\log^{-1}[\log x - s(\log x_i)], \log^{-1}[\log x + s(\log x_i)]]\!]$. Q: NRM/(lab. susc. × H), $H = 0.555$ G; δ: rock density based on 10 measurements per site; A_n: degree of anisotropy; N: number of samples and sites, respectively; D_m and I_m: mean declination and inclination of NRM (*in situ*); k and α_{95}: precision parameter and radius of the 95 per cent confidence circle about the mean direction.

3.4 DEMAGNETIZATION RESULTS

At least one specimen from each site was initially AF demagnetized in 19–28 steps up to maximum fields between 800 and 2200 Oe peak. The results of this pilot demagnetization were analysed using a computer program developed by Stupavsky & Symons (1978). Their

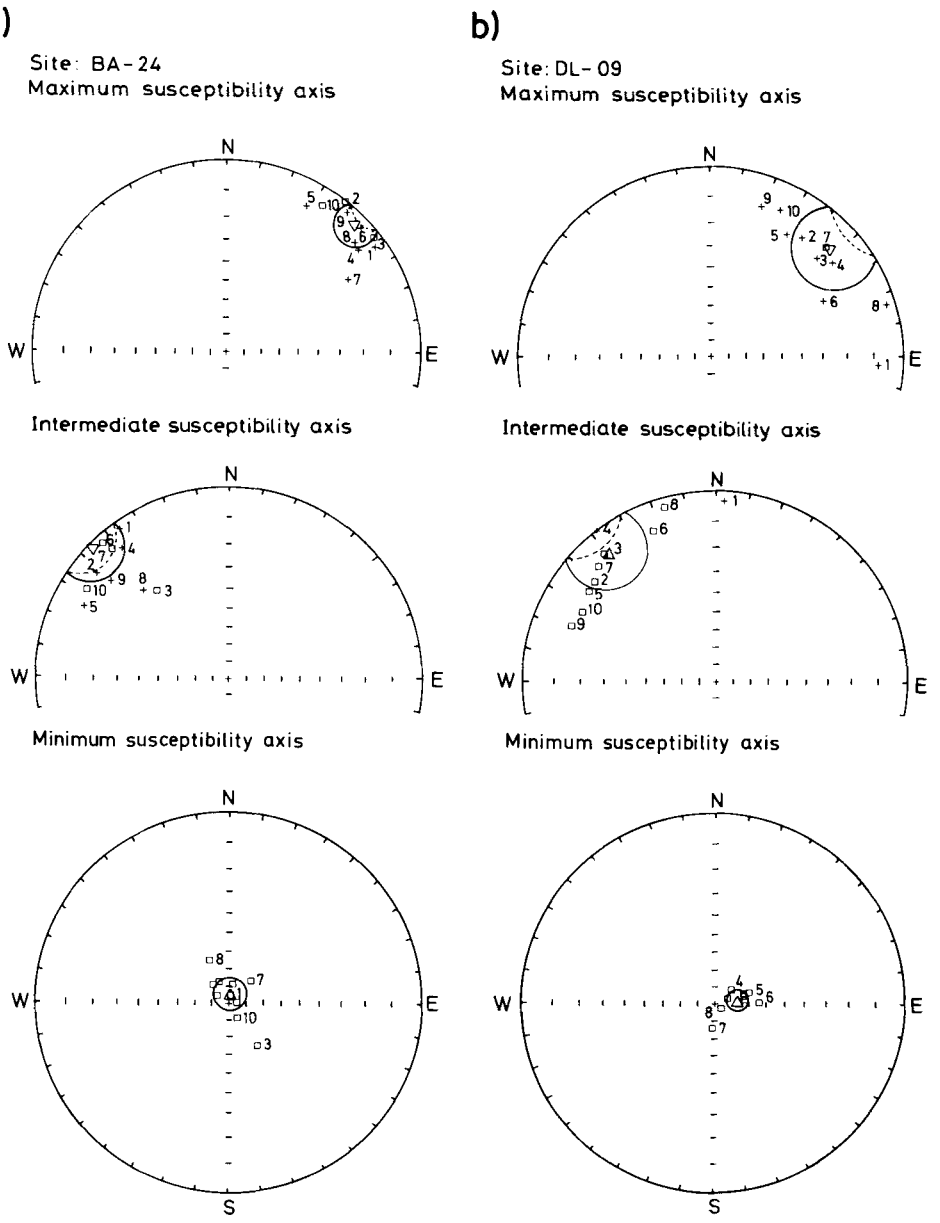

Figure 3. Orientation of the anisotropy ellipsoid for two sites with well-defined axes. Stereographic projection, crosses lower hemisphere (positive inclination), open squares upper hemisphere (negative inclination), triangles mean values (down – positive inclination, up – negative inclination), circle of 95 per cent confidence about the mean. The maximum axis is related to the flow direction of the magma, whereas the minimum axis is perpendicular to the flow plane (see text).

stability index (PSI) proved to be very useful in selecting the optimum cleaning fields, whereas their least-squares modelling programme was unstable due to noise in the AF demagnetization data (acquisition of ARM at high AF fields). The optimum AF field was chosen to be the AF step with the lowest PSI index.

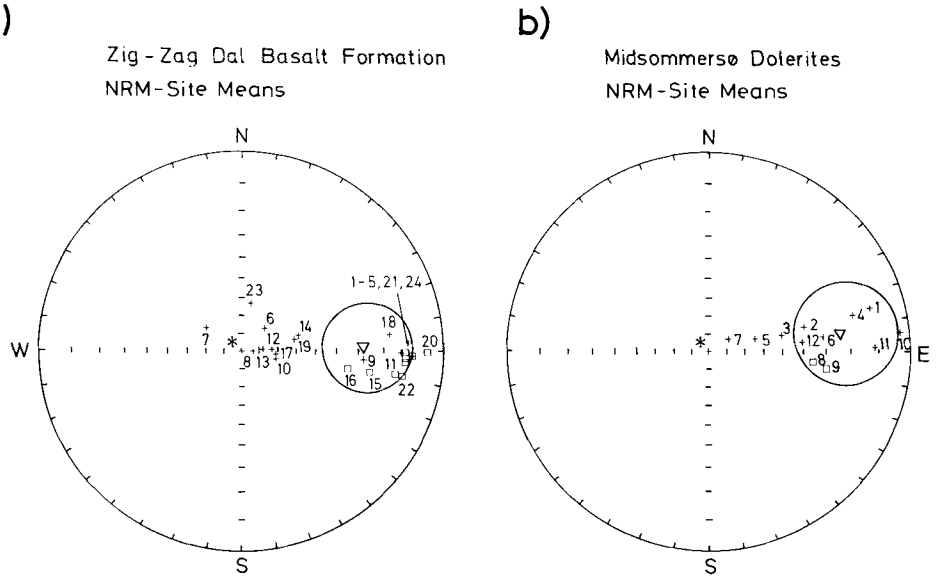

Figure 4. Site mean values of the NRM directions (*in situ, cf.* Table 1) for the two rock types. Symbols as in Fig. 3. The numbers are site numbers, the asterisk indicates the present Earth field direction. The NRM directions appear to be scattered along two east–west, approximately vertical great circles, indicating that the resulting NRM is composed of at least two components, a soft viscous component (in the present field direction) and a more stable, perhaps primary magnetization. Note that sites with high Q-value tend to have low or negative inclination values.

In Figs 5(a)–8(a) some typical results of the pilot demagnetizations are shown. On the basis of these results the sites from the two rock types may be divided into three categories:

1 Stable sites

The majority (2/3) of all sites has pilot specimens which yield a single characteristic remanence direction after removal of secondary components. Fifteen sites in the basalts and nine sites in the dolerites show this behaviour.

In this category we find two subgroups:

(a) Very stable specimens with typical 'knee shaped' intensity decay curves and a very small secondary component (Fig. 5a).

(b) Stable specimens with a significant secondary component in the direction of the present Earth field and a rapid decrease in the intensity during the first few AF steps due to the removal of this component (Fig. 6a).

2 Intermediate sites

The direction of magnetization of the majority of pilot specimens from these sites moves along a great circle path towards a lower inclination. No stable end points are reached because the remanence at higher fields is dominated by ARM, introduced under the demagnetization (Fig. 7a). A few pilot specimens from these sites show the same behaviour as specimens from category (1b). Four sites from the basalts and one dolerite sites belong to this category.

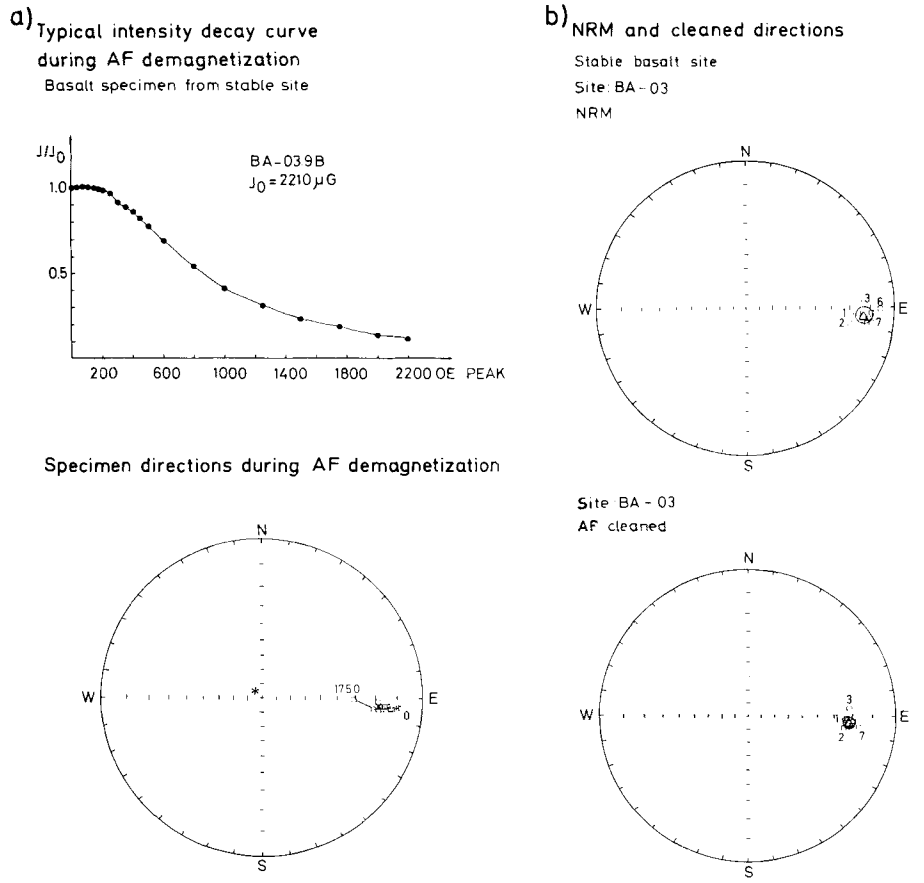

Figure 5. (a) Detailed AF demagnetization experiment with a basalt pilot specimen from a stable site, showing a typical 'knee-shaped' intensity decay curve and very stable directions under demagnetization. Numbers indicate different AF steps in Oe. (b) The NRM and cleaned directions for all samples from the same site, showing very little within site scatter. Numbers are sample numbers. (Symbols as in Fig. 3.)

3 Unstable sites

These sites (two sites in the dolerites and five sites in the basalts) show a very rapid decrease in the intensity. No indication of a stable remanent magnetization other than the NRM is found. The remanence is totally dominated by a viscous magnetization in the present Earth field direction (Fig. 8a).

After pilot demagnetization the subsequent bulk demagnetization was carried out. For each site one specimen from each sample was demagnetized in four to eight steps around the optimum cleaning field. These investigations confirm the results of the pilot demagnetization (see Figs. 5b to 8b). The intermediate sites also yield fairly stable directions. Table 2 gives the mean values and Fisher statistics of the demagnetization results together with the median destructive field ($H_{1/2}$) and the optimum cleaning field (H^*). The stable directions for both rock types show an easterly declination (between 75.5° and 103.4°) and a negative inclination (−1.5° to −42.1°). In most cases the site mean direction with the lowest α_{95}-value was chosen as the optimum stable direction, assuming similar magnetic properties for all specimens from one site. A few specimens were omitted from a site mean mostly due to orientation errors or strong alteration/weathering. These edited sites are marked with ED in

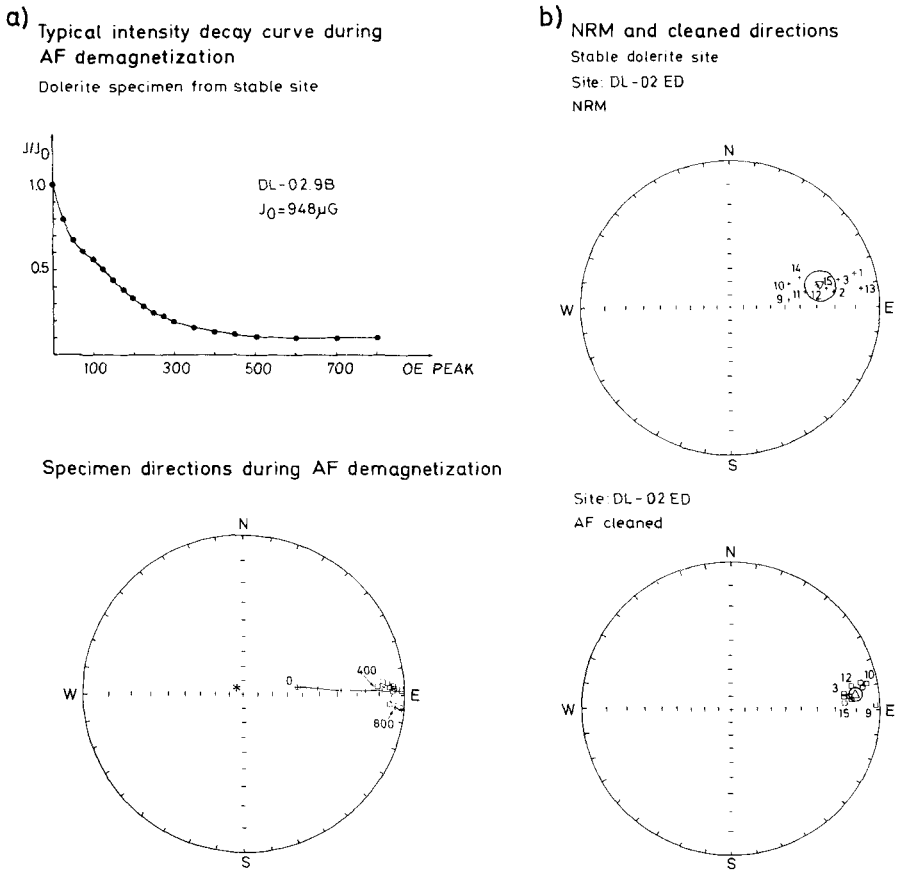

Figure 6. (a) Dolerite pilot specimen from a stable site with rapid decrease in the intensity during the first few AF steps, while the direction moves along a great circle towards a stable end-point due to the removal of a secondary component in the present Earth field direction. (b) The NRM and cleaned directions showing a shift in inclination from positive to negative values. (Symbols as in Fig. 3, numbers as in Fig. 5.)

Table 2. The specimens at four sites in the basalt and one site in the dolerites showed a different behaviour during the AF demagnetization. The PSI index for these specimens was used to find the individually most stable directions. These directions were then combined using Fisher statistics to give site mean values. The five sites are marked with BEST in Table 2. The editing did not change the general result but improved the statistics.

3.5 CURIE TEMPERATURES AND OPAQUE MINERAL PETROLOGY

Thermomagnetic curves (Fig. 9) were measured in air on 14 powder samples from 14 sites using a low field bridge type instrument (susceptibility versus temperature), whereas six measurements were made on samples from four sites using the J_s/T method (saturation magnetization versus temperature). The Curie temperatures (T_c) are listed in Table 2 for the stable sites. Five samples show more than one Curie temperature. Kink effects and inflection points (Ade-Hall, Palmer & Hubbard 1971) have been seen for a few samples.

Twenty-four polished sections from 20 sites were prepared and examined under the ore microscope (maximum magnification x 625). Only qualitative results were obtained. The

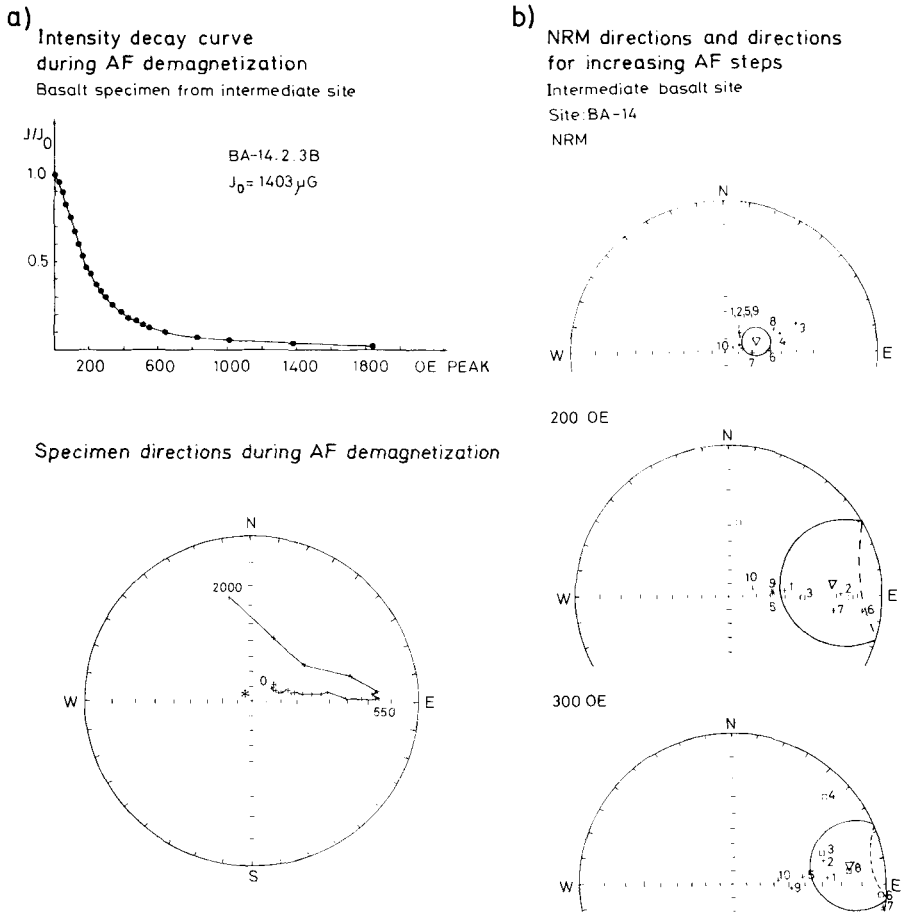

Figure 7. (a) Pilot specimen from an intermediate basalt site where the direction moves under the demagnetization along a great circle path towards lower inclination. No stable end-points are reached. (b) NRM directions and directions for increasing AF steps. (Symbols as in Fig. 3, numbers as in Fig. 5.)

investigated polished sections can roughly be divided into two groups, each containing two subgroups.

Group 1 show skeletal titanomagnetite crystals with high Fe-content and no visible exsolution (site BA-01, 02, 24). The T_c-values lie between 450 and 470°C. Some sites, all from the Basal Unit of the basalts (BA-18, 20, 22) show skeletal grains of relict magnetite now nearly completely altered to hematite. These sites show at least two Curie temperatures, one between 440 and 460°C and the other between 540 and 590°C.

The polished sections in group 2 exhibit titanomagnetite crystals with exsolution lamellae of ilmenite. The ilmenite is nearly completely altered (oxidized) to hematite and rutile, whereas the Fe-rich phase (nearly pure magnetite) is partly altered corresponding to the oxidation stage C4 to C6 (Haggerty 1976). Sites BA-04, 11, 14 (?), 15, 23; DL-01, 06, 09, 10, 11 belong to this group. Sites BA-07 and 08 show completely altered titanomagnetite with ghost structures after ilmenite lamellae. Samples from group 2 have T_c-values between 550 and 580°C.

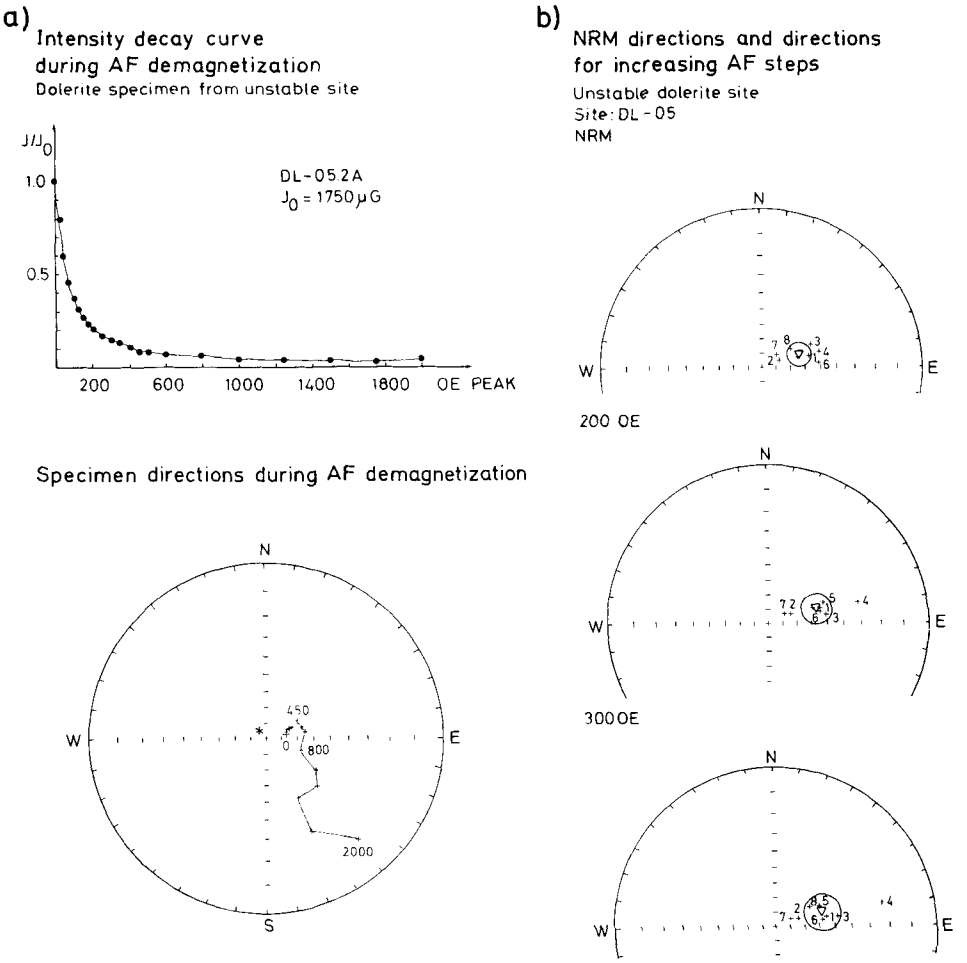

Figure 8. (a) Pilot specimen from an unstable dolerite site showing rapid decrease in the intensity. The magnetization is dominated by a viscous magnetization in the present field direction. (b) Sample directions for the same site. No stable remanent magnetization other than the NRM is found. (Symbols as in Fig. 3, numbers as in Fig. 5.)

4 Discussion of the palaeomagnetic results

4.1 THE PRIMARY MAGNETIZATION

The NRM of the stable sites consists of a stable-primary-component and an unstable-secondary-component in the present Earth field direction (Fig. 4). The AF-demagnetization experiments uncovered only one stable component of the remanence with eastward declination and negative inclination (Fig. 10). The normalized decay curves for these specimens (Figs 5a and 6a) suggest that the stable magnetization is of thermoremanent or thermochemical remanent origin. It is not possible from the decay curves to distinguish between these two types of magnetization.

On the basis of the demagnetization experiments the following conclusions about the nature of the primary magnetization seem reasonable:

The median destructive field ($H_{1/2}$) varies considerably through the basalt sequence. Sites with high intensity and susceptibility values, indicating a high content of magnetite, show

Table 2. (a) Zig-Zag Dal Basalt Formation, palaeomagnetic results.

Site	N	T_c	$H^{\#}$	$H_{\frac{1}{2}}$	D_m	I_m	k	α_{95}	Pole position		δ_m	δ_p
		°C	(Oe)	(Oe)	(°)	(°)		(°)	Lat.(°S)	Long.(°E)	(°)	(°)
BA-01 ED	9(10)	470	100	86±7	91.2	-14.3	801	1.8	7.3	64.8	1.8	0.9
BA-02 ED	9(10)		100	96±17	92.4	-15.0	461	2.4	7.9	63.8	2.4	1.2
BA-03	9		800	1006±253	94.1	-23.8	419	2.5	12.9	62.8	2.7	1.4
BA-04 ED	9(10)	570,580	500	946±331	91.7	-24.0	677	2.0	12.6	65.2	2.1	1.1
BA-05	10		500	1194±549	93.9	-22.8	496	2.2	12.3	63.0	2.3	1.2
BA-06 BEST	6(10)	515	300-450	40±6	87.5	-19.7	38	11.1	9.6	69.0	11.6	6.1
BA-09 BEST	9		500-600	1021±210	97.0	- 6.4	298	3.0	4.2	58.6	3.0	1.5
BA-10 BEST	8(9)		75-200	42±10	102.7	- 9.7	327	3.1	6.7	53.2	3.1	1.6
BA-11	9	570	500	657±270	97.7	-25.8	4037	0.8	14.5	59.5	0.9	0.5
BA-14 BEST	6(10)	425,545,580	450-700	382±168	90.4	-15.2	12	20.4	7.7	65.4	20.9	10.8
BA-15	10	565	500	434±117	100.7	-32.1	516	2.1	18.8	56.4	2.4	1.3
BA-16	10		600	598±123	101.8	-41.0	218	3.3	25.6	56.8	4.0	2.4
BA-18	3	440,570	700	1228±257	89.0	-36.2	54	16.9	19.7	68.7	19.7	11.4
BA-19	4		800	424±69	84.9	- 1.5	39	15.0	3.0	69.6	15.0	7.5
BA-20 ED	2(3)		700	574±126	90.1	-42.1	288	14.7	24.0	68.4	18.1	11.1
BA-21 ED	2(3)		800	803±296	103.4	-36.8	268	15.3	22.3	54.5	17.9	10.5
BA-22	3	460,540,590	800	533±116	100.7	-25.8	103	12.2	15.0	56.1	13.2	7.1
BA-23 ED	7(10)		175	77±21	79.2	- 5.8	288	3.6	1.2	75.6	3.6	1.8
BA-24	10	450	500	173±15	94.2	-18.0	232	3.2	9.7	61.8	3.3	1.7
Porphyritic	10(12)				94.8	-19.4	81	5.4	10.6	61.6	5.6	2.9
Aphyric	4(7)				90.6	-20.1	22	19.9	10.3	65.5	20.8	10.9
Basal unit	5(5)				93.4	-28.8	21	16.9	15.7	63.6	18.6	10.2
All sites	19(24)				93.6	-22.0	37	5.5	11.8	63.0	5.8	3.1

(b) Midsommersø Dolerites, palaeomagnetic results.

Site	N	T_c	$H^{\#}$	$H_{\frac{1}{2}}$	D_m	I_m	k	α_{95}	Pole position		δ_m	δ_p
		°C	(Oe)	(Oe)	(°)	(°)		(°)	Lat.(°S)	Long.(°E)	(°)	(°)
DL-01	10		250	427±130	75.5	-14.4	74	5.6	5.3	69.2	5.7	2.9
DL-02 ED	10(13)	550	200	160±20	83.2	-10.4	183	3.6	4.2	61.3	3.6	1.8
DL-03 ED	7(9)		150	166±151	80.1	- 9.1	55	8.2	3.2	64.3	8.3	4.2
DL-04 ED	9(10)		175	218±46	79.0	- 8.6	220	3.5	2.8	65.3	3.5	1.6
DL-06	9	560	450	166±25	82.9	-12.1	240	3.3	5.1	61.7	3.4	1.7
DL-08	10	565	300	227±34	101.4	-35.5	251	3.0	21.0	53.5	3.5	2.0
DL-09	10	510,560	150	213±13	101.8	-28.6	662	1.8	16.8	52.3	2.0	1.1
DL-10	12	520,555	400	305±64	84.4	-12.5	114	4.1	5.4	65.6	4.2	2.1
DL-11 BEST	12	570	200-800	741±481	90.9	-10.3	81	4.8	5.2	59.0	4.9	2.5
DL-12	11		1000	1286±1656	81.5	- 2.6	68	5.6	0.1	67.7	5.6	2.8
Loc.1	5(6)				80.1	-10.9	438	3.6	4.1	64.4	3.6	1.8
Loc.3	2(2)				101.6	-32.0	275	15.1	18.9	52.9	17.0	9.6
Loc.4	3(3)				85.5	- 8.4	133	10.7	3.6	64.1	10.8	5.4
All sites	10(12)				85.6	-14.5	39	7.8	6.6	63.2	8.0	4.1

Notes:
N: number of accepted samples (sites), total number of samples (sites) in parenthesis; T_c: Curie temperature; $H^{\#}$: optimum cleaning field; $H_{1/2}$: median destructive field picked from intensity decay curves; D_m and I_m: mean declination and inclination of the stable remanence direction (bedding corrected); k and α_{95}: precision parameter and radius of the 95 per cent confidence circle about the mean direction. The palaeomagnetic pole positions are calculated from the site mean directions and group mean directions respectively. δ_m and δ_p: semi-axes of the 95 per cent confidence oval about the pole. The geographical mean coordinates of the basalt sites are 81.2°N, 25.2°W and of the dolerite sites, 81.8°N, 32.2°W.

low $H_{1/2}$-values (*c.* 85–175 Oe), which suggests that the main part of the remanence is carried by multi-domain grains, whereas the stable component – stable up to fields of *c.* 500 Oe – resides in single-domain grains [sites BA-01, 02, 24, 10(?), 06(?)]. Polished sections from some of these flows show optically homogeneous titanomagnetites with a skeletal shape indicating a very rapid cooling (quenching) of these flows. The titanomagnetite, probably with a high Fe-content up to nearly pure magnetite, appears to be very little altered.

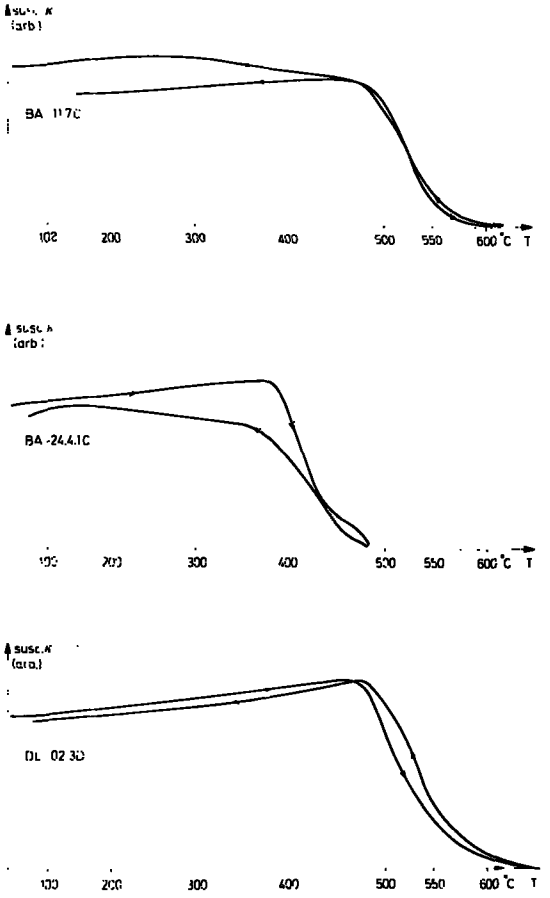

Figure 9. Typical examples of susceptibility versus temperature (in air) of powder specimens. The upper and lower curve indicate the presence of hematite in the measured specimens, whereas the middle curve is due to titanomagnetite with high Fe-content. The latter curve is from a basalt site with typical skeletal grains of titanomagnetite.

Basalt sites with medium to high intensity and susceptibility values and high $H_{1/2}$-values (*c.* 430–1000 Oe) show extremely stable directions up to AF-fields of 1500–2000 Oe peak [sites BA-03–05, 11, 15, 16, 9(?)]. Since multi-domain grains cannot withstand AF-fields greater than 800 Oe (Evans & McElhinny 1969), the very high $H_{1/2}$-values indicate that the remanence of these sites is mainly carried by single-domain or pseudo-single domain grains of almost pure magnetite. The presence of almost pure magnetite is also suggested by T_c-values of about 570°C at these sites. The polished sections show oxidized titanomagnetites. A high temperature deuteric oxidation process may account for the formation of the single- and/or pseudo-single domain grains on a submicroscopical scale.

Sites in the Basal Unit of the basalts reveal two or three different Curie temperatures (*c.* 420, 540, 590°C), which indicate the presence of more than one magnetite phase, probably Fe-rich titanomagnetites and hematite. The $H_{1/2}$-values are generally high (420–1230 Oe). Polished sections from some of these sites show that hematization is widely developed, also indicated by low values of intensity and susceptibility. The hematite is probably formed during secondary alteration processes. Kalsbeek & Jepsen (1983) relate this

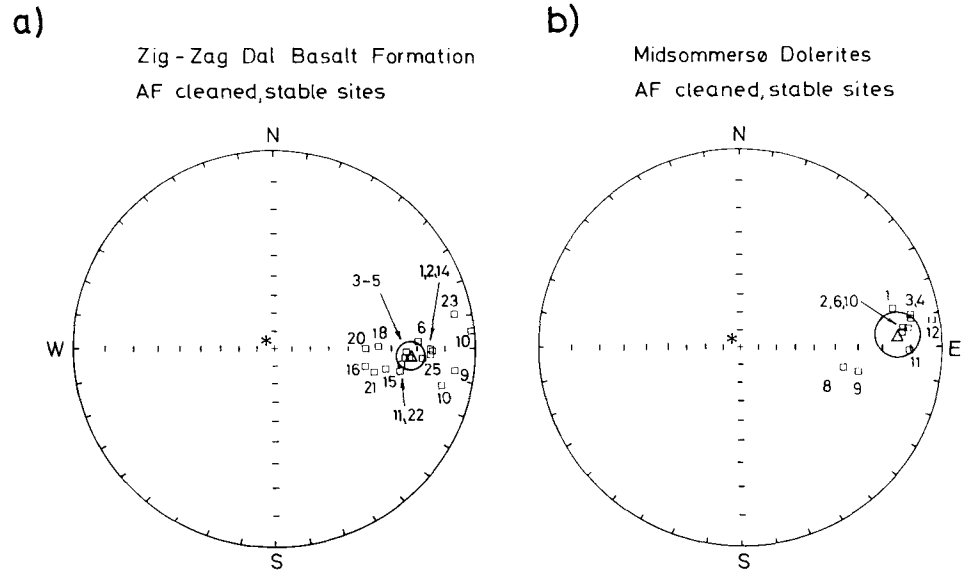

Figure 10. AF cleaned optimum site mean directions from all stable sites in the basalts and the dolerites respectively. Symbols as in Fig. 3. Some directional streaking can be seen for the basalts whereas the dolerite sites clearly fall into two groups, one consisting of sites from locality 3 (DL-08, 09) and the other of sites from localities 1 and 4.

alteration with the likely subaqueous effusion mode of the Basal Unit. The formation of the hematite is therefore most likely contemporaneous with the effusion and cooling of these lava flows.

The intrusion of the dolerites was accompanied by circulating hydrothermal systems, which make deuteric alteration of the dolerites at the time of intrusion very likely. The dolerites show no greater variation in the $H_{1/2}$-values (except DL-11, 12) and Curie temperature, whereas the intensity and susceptibility values vary considerably due to higher alteration (site DL-01) or higher magnetite content (DL-08, 09). In general the remanence is associated with small single or pseudo-single domain grains of almost pure magnetite.

The remanence of the unstable sites is clearly dominated by a viscous component in the present Earth's field direction probably residing on multi-domain grains. These sites show low $H_{1/2}$-values (35–146 Oe) and intermediate Curie temperatures (520–560°C, not listed in Table 2). The unstable nature of the remanence may be explained by extensive weathering found at these sites (BA-07, 08, 12, 13, 17, DL-05, 07).

The stable component of the remanence we identify as the primary component related to the Earth's magnetic field at the time of the intrusion of the dolerites and the effusion of the basalts, since there is *no* geological evidence for later deformation or major alteration of the basalts and dolerites, which could have given rise to remagnetization.

4.2 THE ANISOTROPY DATA

The degree of anisotropy at all sites fall between 1.03 and 1.15 (*cf.* Table 1, except site DL-07), which implies that the theoretical maximum deflection of the magnetization due to the anisotropy is less than 4° (McElhinny 1973). The actual value for the individual sites is certainly less than this value, since the direction of the ancient magnetic field does not lie in the plane containing the maximum and minimum susceptibility axes.

Only a few studies of the magnetic anisotropy in undeformed basalt flows and dolerite intrusions are found in literature (Khan 1962; Wing-Fatt & Stacey 1966; Halvorsen 1974; Ellwood 1978; Thorning & Abrahamsen 1980; see also Hrouda 1982) relating magnetic anisotropy to the flow direction of the magma. The minimum axis is in these studies always found to be normal to the flow plane. Khan (1962) suggested that the intermediate axis is parallel to the flow direction, whereas Wing-Fatt & Stacey (1966), Halvorsen (1974) and Thorning & Abrahamsen (1980) found that the maximum axis defines the flow direction.

A tentative interpretation of the present anisotropy data from sites with well-defined axes and a correlation with geological evidence may be summarized in the following way:

The minimum axis of the anisotropy ellipsoid is generally vertical for the basalt sites. This implies that the flow plane is nearly horizontal, which is most pertinent for flood basalts. Three sites in the basalts (BA-01, 02, 24 – Fig. 3) have well-defined axes with vertical minimum axes. Their maximum axes have a NE–SW direction, probably the flow direction at these sites.

Three sites at the dolerite locality 1 (a major sill) show well-defined axes with nearly vertical maximum axes, suggesting vertical flow. The two site at Hagen Brae (locality 3) also gave consistent results: site DL-08, a feeder dyke to a large sill dipping *c.* 40°SW, has a maximum axis in a SW–NE direction (215°) and the flowplane has a dip of *c.* 42° as deduced from the direction of the minimum axis. The second dyke, dipping 5–10°SW (site DL-09), has a maximum axis in a NE–SW direction (*c.* 229°) and the flow plane has a dip of *c.* 14° (Fig. 3). These two results are in excellent agreement with geological evidence for the flow direction and the dip of the flow plane of these dykes if it is supposed, that the maximum axis is parallel to the flow direction. The sites at locality 4 (a sill) show no systematic pattern. A possible explanation may be that the laminar flow in the sill had ceased before crystallization in contrast to the dykes.

In conclusion, the results from the dolerite sites support the results of Wing-Fatt & Stacey (1966), Halvorsen (1974) and Thorning & Abrahamsen (1980) suggesting that the maximum axis of the anisotropy ellipsoid is orientated in the flow direction and the minimum axis is perpendicular to the flow plane.

4.3 PALAEOMAGNETIC POLE POSITIONS

The bedding-corrected optimum directions, obtained by the methods outlined previously, are shown in Fig. 10 (*cf.* Table 2). In the basalts some directional streaking is still seen, probably due to imperfect removal of the secondary component in the present Earth field direction. Nevertheless there is no linear relationship between the inclination I_m and the precision parameter k.

The dolerite sites fall clearly into two groups where the two sites from locality 3 (at Hagen Brae) have more steeply inclined directions.

In Table 2 mean directions, Fisher statistics and resulting palaeopoles of the AF-cleaned stable remanent magnetization for all stable sites are compiled, together with the mean values for the three basalt units and the three dolerite localities.

No reversals of the geomagnetic field are recorded in the basalt sequence as, e.g. found for the Proterozoic (*c.* 1300 Ma) Gardar lavas in SW Greenland (Piper 1977a). This may be explained either by the nature of the Proterozoic Earth magnetic field (long stable periods) or by the relatively short timespan of magmatic activity represented by the basalts and dolerites of the present investigation. In the latter case the variation in inclination (±15°) and declination (±10°) may represent a secular variation during effusion of the basalts, i.e. equivalent to or slightly higher than present time equatorial secular variation.

There is no significant ($P = 0.95$; Watson 1956; Watson & Irving 1957) difference between the mean pole positions for the three basalt units. The altered Basal Unit has the same stable direction as the other two units, indicating that the alteration was contemporaneous with the subaqueous effusion of the unit.

The mean pole position for the two dolerite sites at locality 3 differs significantly ($P = 0.95$) from the pole positions for the two other stable localities. Two possible explanations may account for this difference:

(1) The direction of the remanence for the sites at localities 1 and 4 may be biased towards less negative inclination by failure to remove the secondary component completely in the cleaning process.

(2) The intrusion of the two dykes at locality 3 may have taken place at a different time during the period of intrusive activity as also indicated by slightly different age determinations (Jepsen & Kalsbeek 1979). The suggested secular variation seen in the basalt sequence thus may account for a change of 10–20° of the individual pole position.

In Table 3 the mean palaeomagnetic poles for the two rock types are listed. They were obtained using Fisher statistics on the pole positions for the individual sites (McElhinny 1973) to avoid errors due to the geographical spread of the dolerite localities. There is no significant ($P = 0.95$) difference between the two pole positions indicating that the basalts and the dolerites are contemporaneous and hence very likely genetically related.

The mean pole position for the basalt sequence most likely represents a true palaeomagnetic pole position due to the averaging of the timespan in which the magmatic activity lasted. The dolerite pole position is more difficult to evaluate; it is, however, suggested that this pole is also a true palaeomagnetic pole due to the duration of the intrusive activity.

4.4 COMPARISON WITH A RELEVANT NORTH AMERICAN APW-CURVE

In order to be able to compare the two mean poles for the basalts and the dolerites with a relevant North American APW-curve the pole positions have been corrected for an assumed Phanerozoic drift (i.e. the opening of the Davis Strait) using the continental reconstruction of Bullard, Everett & Smith (1965).

In Fig. 11 the two rotated pole positions (poles ZBA and MDL, *cf.* Table 3) are plotted in a recently proposed APW-curve for Laurentia for the time interval 1.1–1.5 Ga (Berger & York 1980). The curve is based on 36 reliable poles (Table 4) and has a width of *c.* 15°. The most reliably dated magnetizations are *c.* 1200 Ma for the Sudbury dykes (pole 18), Mackenzie diabase (pole 19) and Muskox intrusions (pole 20). Less certain tiepoints are

Table 3. Mean palaeomagnetic pole positions.

Rock type	No. of sites	No. of samples	Pole position before rotation		Pole position after rotation		K	A_{95}
			Lat.	Long.	Lat.	Long.		
Basalts	19 (24)	135	12.2°S	62.8°E	15.3°S	47.0°E	76	3.8°
Dolerites	10 (12)	100	6.9°S	62.0°E	10.1°S	45.8°E	88	5.1°

Notes:
Mean pole positions calculated from site mean pole positions. Number of stable sites with total number of sites sampled in parentheses. K and A_{95}: precision parameter and radius of 95 per cent confidence circle about the mean pole (Fisher 1953; McElhinny 1973). Rotation of Greenland to North America: 18° clockwise about an Euler pole at 70.5°N, 94.4°W (Wells & Verhoogen 1967).

Table 4. Palaeopoles for Fig. 11.

Pole	Name	Ref	B	N	Tr	Pole position Lat.(°N)	Long.(°E)	K	A_{95} (°)	δ_m (°)	δ_p (°)	Age
1	Iron mountain primary ore, Missouri	1,298	0	25	A	30.7	42.7	0	0	0	0	
2	Pioneer shale, Arizona	2	0	25	T	32.0	46.0	0	0	2.6	1.4	1300 - 1350 Ma
3	Sibley red beds, Arizona	1,473	7	25	T	21.0	36.0	0	0	13.0	7.0	Rb/Sr: 1340±32 Ma
4	Belt Series, Alberta - Montana	3	15	47	T	17.1	37.8	0	0	7.1	4.1	1100 - 1325 Ma
5	Belt Series, Montana	1,300	0	0		12.8	30.4	37	8.5	0	0	1100 - 1325 Ma
6	Sherman granite, Colorado	1,172	5	14	A	8.0	29.0	0	0	6.0	4.0	c. 1410 Ma
7	Mistastin pluton, Labrador	4	7	35	A	1.0	21.5	64	7.6	0	0	Rb/Sr: 1318±30 Ma
8	Harp Lake complex, Labrador	5	24	110	A+T	- 2.0	25.4	0	0	6.1	3.0	c. 1450 Ma
9	St. Francois rocks, Missouri	1,241	6	144	A	1.3	36.1	0	0	9.6	6.1	c. 1375 Ma
10	Michikamau intrusions, Labrador	6	12	54	A+T	1.5	38.0	103	4.5	0	0	1400 - 1460 Ma
11	Croker Island complex, Ontario	1,129	19	23	A	- 5.4	37.2	0	0	10.5	6.7	c. 1475 Ma
12	Shefferville dikes, Labrador	7	4	15	A	-11.0	43.5	1033	2.2	0	0	K/Ar: 1255±52 Ma 1146±104 Ma
GLL	Gardar lavas, lower group, Greenland	8	7	34	A+T	-10.6	42.8	0	0	14.1	7.6	c. 1300 Ma
GLU	Gardar lavas, upper group, Greenland	8	24	113	A+T	-20.4	26.3	0	0	9.0	4.8	c. 1300 Ma
13	Harp dikes, Labrador	5	3	14	A	-17.1	49.0	0	0	9.0	5.6	c. 1350 Ma K/Ar: 1316±94 Ma
14	Harp Lake marginal rocks, Labrador	5	6	22	A	-13.9	35.9	0	0	10.7	5.9	
BD_o	BD_o dykes, Greenland	9	2	14	A	-14.9	31.0	0	0	14.5	7.6	Rb/Sr: 1217±18 Ma 1212±18 Ma
15	Badcall dyke, Scotland	10	1	32	A	- 8.3	32.6	0	0	4.4	2.2	c. 1440 Ma
16	Nain anorthosite complex, Labrador	11	21	101	A+T	-11.7	30.0	0	0	3.1	1.6	c. 1400 Ma
17	Seal Lake group redbeds, Labrador	1,464	10	45	T	- 6.0	25.0	0	0	6.0	3.0	c. 1300 Ma (ref. 9)
18	Sudbury dykes, Ontario	12,13	38	0	A	2.9	13.1	51	3.3	0	0	Rb/Sr: 1194 - 1219 Ma
19	Mackenzie diabase, N.W.T.	1,453	47	0	A	- 1.4	9.5	75	2.4	0	0	Rb/Sr: 1204 - 1251 Ma (ref. 13)
20	Muskox intrusion, N.W.T.	1,115	80?	19	A	- 4.0	5.0	0	0	19.0	11.0	c. 1250 Ma (ref. 9)
ALP	Arsuk lamprophyres, Greenland (pole 21)	13, 9	9	51	A	- 8.8	9.0	0	0	10.1	5.1	Rb/Sr: 1228 - 1249 Ma
KRD	Kûngnât ring dykes, Greenland (pole 22)	13, 9	4	18	A	- 9.2	1.9	0	0	2.3	4.4	Rb/Sr: 1203 - 1254 Ma
ID	Ivigtut dolerites, Greenland (pole 24)	13, 9	24	138	A	-14.5	5.0	0	0	9.4	4.7	Rb/Sr: 1237 - 1250 Ma
25	South Trap Range, normal, Michigan	1,374	7	36	A	- 9.8	19.6	0	0	13.5	7.8	c. 1200 Ma (ref. 9)
26	Isle Royal, upper flows, Minnesota	1,379	5	24	A	-25.9	24.3	0	0	13.8	9.7	
27	Aillik dikes, Labrador	1,353	6	32	A	-27.0	44.0	64	7.1	0	0	1000 - 1100 Ma
28	South Trap Range, reversed, Michigan	1,150	14	61	A	-28.0	52.5	0	0	7.9	6.8	c. 1220 Ma
29	Alona Bay lavas, Ontario	1,139	1	11	A	-47.4	52.7	0	0	18.5	17.1	
30	Mamainse-Gargantua lavas reversed, Ontario	1,395	12	67	A+T	-48.5	52.0	0	0	16.0	14.0	
31	Logan diabase, reversed Ontario	1,309	0	0		-48.4	37.5	108	7.4	0	0	c. 1160 Ma (ref. 12)
HGD	Hviddal giant dykes, Tugtutôq, Greenland	14	7	38	A	-38.3	20.6	0	0	12.2	7.6	Rb/Sr: 1175±9 Ma
GGD	Gabbro giant dykes, Gardar, Greenland (pole 32)	8,14	13	73	A	-46.7	33.1	0	0	11.1	8.0	1168 - 1175 Ma
NGU	Narssaq gabbro + ultramafics, Greenland	14	4	22	A	-36.1	31.1	0	0	12.1	7.8	1168 - 1175 Ma
NED	NE-dykes, Tugtutôq, Greenland	9	47	264	A	-41.0	30.0	0	0	6.1	4.1	1168±37 Ma
33	Mamainse lavas, reversed Ontario	1,140	20	20	A	-54.4	32.4	0	0	12.8	10.6	c. 1076 Ma
34	Mamainse lavas, normal, Ontario	1,141	52	52	A	-36.8	0.4	0	0	5.3	3.5	c. 1076 Ma
35	Logan dykes, normal, Ontario	1,268	15	69	A	-35.0	1.0	0	0	7.0	4.0	c. 1160 Ma (ref. 12)
36	Mamainse-Gargantua lavas normal, Ontario	1,394	15	76	A+T	-29.5	2.7	0	0	7.6	4.4	Rb/Sr: 1050±50 Ma
IMS	Ilímaussaq, marginal syenites, Greenland	15	5	31	A	-38.7	75.6	0	0	18.9	16.2	
IFR	Ilímaussaq, fractionated rocks, Greenland	15	6	32	A	-75.5	60.4	0	0	41.0	37.1	Rb/Sr: 1143±21 Ma 1126±28

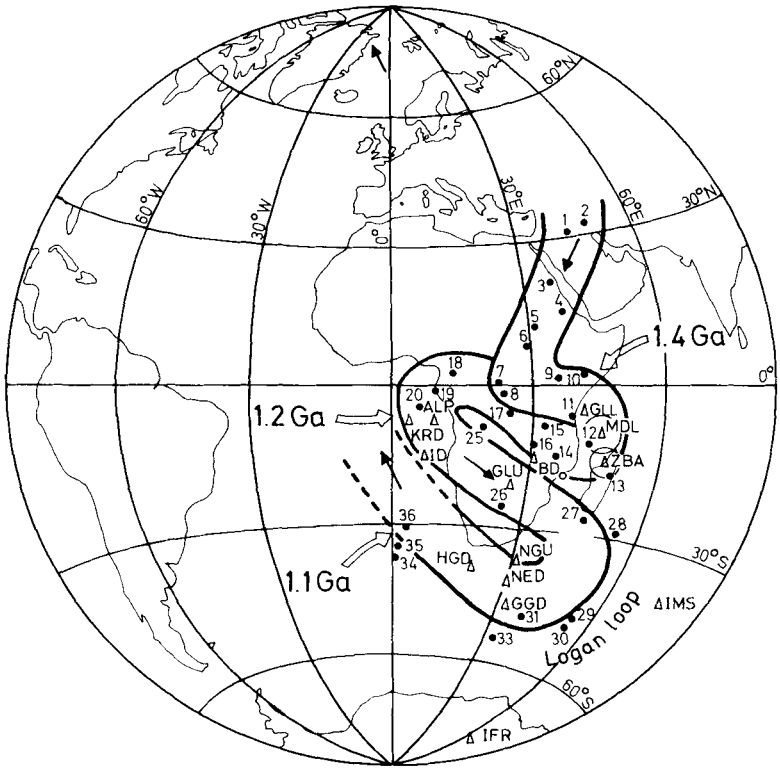

Figure 11. A North American APW-curve (Berger & York 1980) for the time interval 1.1–1.5 Ga. The curve has a width of *c.* 15° and is based on 36 reliable palaeopoles (*cf.* Table 4). The poles from Greenland are marked with triangles and they are corrected for Phanerozoic drift of Greenland according to Bullard *et al.* (1965) continental reconstruction. ZBA mean pole position for the Zig-Zag Dal Basalt Formation (*cf.* Table 3), MDL mean pole position for the Midsommersø Dolerites (*cf.* Table 3). The circles of 95 per cent confidence are shown for these two poles.

shown at *c.* 1.1 and 1.4 Ga. Berger & York (1980) prefer to plot the poles near the present-day Atlantic rather than in the Pacific hemisphere as older APW-curves. This choice permits the shortest connection between the Grenvillian and Cambrian poles. The Greenlandic poles, marked with triangles in Fig. 11, are corrected for Phanerozoic drift.

The two pole positions derived in this study fall between 1.2 and 1.4 Ga. The nearest poles have ages between 1250 and 1350 Ma (poles 12 and 13). Pole GLL from the Gardar lavas of South Greenland is not significantly different from the two poles from North Greenland. This suggests a palaeomagnetic age for the basalts and the dolerites between 1250 and 1350 Ma, which is in good agreement with the radiometric age found for the dolerites.

Notes:

References: 1, Irving & Hastie (1975 – listing numbers in the Ottawa Catalogue). 2, Scott (1976). 3, Evans, Bingham & McMurry (1975). 4, Fahrig & Jones (1976). 5, Irving, Emslie & Park (1977). 6, Emslie, Irving & Park (1976). 7, Fahrig (1976), 8, Piper (1977a), 9, Piper & Stearn (1977). 10, Beckmann (1976). 11, Murthy (1978). 12, Palmer, Merz & Hayatsu (1977). 13, Patchett, Bylund & Upton (1978). 14, Piper (1977b). 15, Piper (1976). *B*: number of sites; *N*: number of samples; Tr: laboratory treatment (A–AF demagnetization, T – thermal demagnetization); pole positions and statistical parameters from Fisher statistics; age: age determinations from various sources and variable reliability (^{87}Rb decay constant: 1.42×10^{-11} yr^{-1}); pole numbers in parentheses refer to Berger & York (1980).

The polarity of the two poles from North Greenland is opposite to the widespread Mackenzie–Mid-Gardar magmatism dated about 1200 Ma (Piper 1977a).

The palaeolatitude of eastern North Greenland at the time of the formation of the basalts and dolerites lies between 7 and 11°S as derived from the palaeoinclinations. Greenland's major geographical axis was orientated nearly E–W. This equatorial position of Greenland lasted according to the APW-curve of Berger & York (1980 and Fig. 11) for the time interval between *c.* 1400 and 1200 Ma.

Except for pole GLU (Fig. 11) from the upper group of the Gardar lavas, the positions of the Greenlandic Upper Proterozoic poles is in good agreement with the APW-curve of Berger & York (1980). This supports the applicability of the continental reconstruction of Bullard *et al.* (1965) to Proterozoic times (Piper 1977a), and also suggests that North America and Greenland formed a single lithospheric unit in the Upper Proterozoic.

Acknowledgments

We wish to thank the staff and colleagues at the Geological Survey of Greenland (GGU), Copenhagen, and at the Laboratory of Geophysics, Aarhus University, for extensive help and discussions. Some of the Curie temperatures were measured by G. Schönharting, Copenhagen. Special thanks are due to L. Thorning and N. Henriksen (both GGU), who made this work possible.

This paper is published with the permission of the Director of the Geological Survey of Greenland.

References

Abrahamsen, N. & Marcussen, C., 1980. Preliminary results of rock- and palaeomagnetic field work in Peary Land, North Greenland, *Rapp. Grønn. geol. Unders.*, **99**, 137–145.

Ade-Hall, J. M. Palmer, H. C. & Hubbard, T. P., 1971. The magnetic and opaque petrological response of basalts to regional hydrothermal alteration, *Geophys. J. R. astr. Soc.*, **24**, 137–174.

Beckman, G. E. J., 1976. A Palaeomagnetic study of part of the Lewisian complex, north-west Scotland, *J. geol. Soc. London*, **132**, 45–59.

Berger, G. W. & York, D., 1980. Reinterpretation of the North American apparent polar wander curve for the interval 800–1500 Ma, *Can. J. Earth Sci.*, **17**, 1229–1235.

Bullard, E. C., Everett, J. E. & Smith, A. G., 1965. The fit of the continents around the Atlantic, *Phil. Trans. R. Soc. A*, **258**, 41–51.

Christie, K. W. & Symons, D. T. A., 1969. Apparatus for measuring magnetic susceptibility and its anisotropy, *Geol. Surv. Can. Pap.*, **69–41**, 1–10.

Clemmensen, L. B., 1979. Notes on the palaeographical setting of the Eocambrian tillite-bearing sequence of southern Peary Land, North Greenland, *Rapp. Grønn. geol. Unders.*, **88**, 15–22.

Collinson, J. D., 1980. Stratigraphy of the Independence Fjord Group (Proterozoic) of eastern North Greenland, *Rapp. Grønn. geol. Unders.*, **99**, 7–23.

Ellwood, B. B., 1978. Flow and emplacement direction determined for selected basaltic bodies using magnetic susceptibility measurements, *Earth planet. Sci. Lett.*, **41**, 254–264.

Emslie, R. F., Irving, E. & Park, J. K., 1976. Further palaeomagnetic results from the Michikamau intrusion, Labrador, *Can. J. Earth Sci.*, **13**, 1052–1057.

Evans, M. E., Bingham, D. K. & McMurry, E. W., 1975. New palaeomagnetic results from the Upper Belt – Purcell supergroup of Alberta, *Can. J. Earth Sci.*, **12**, 52–61.

Evans, M. E. & McElhinny, M. W., 1969. An investigation of the origin of stable remanence in magnetite-bearing igneous rocks, *J. Geomagn. Geoelect., Kyoto*, **21**, 757–773.

Fahrig, W. F., 1976. Palaeomagnetism and age of the Schefferville diabase dykes, *Geol. Surv. Can. Pap.*, **76-1B**, 153–155.

Fahrig, W. F. & Jones, D. L., 1976. The palaeomagnetism of the Helikan Mistastin pluton, Labrador, Canada, *Can. J. Earth Sci.*, **13**, 832–837.

Fisher, R., 1953. Dispersion on a sphere, *Proc. R. Soc. A*, **217**, 295–305.

Haggerty, S. E., 1976. Oxidation of opaque mineral oxides in basalts, in *Oxide Minerals,* vol. 3, pp. 1–100, ed. Rumble, D., III, Mineralogical Society of America, Short Course Notes, November 1976.

Halvorsen, E., 1974. The magnetic fabric of some dolerite intrusions, NE Spitsbergen; implications for their mode of emplacement, *Earth planet. Sci. Lett.,* **21,** 127–133.

Henriksen, N., 1981. Systematic 1:500.000 mapping in the Peary Land region, North Greenland, *Rapp. Grønn. geol. Unders.,* **105,** 9–14.

Hrouda, F., 1982. Magnetic anisotropy of rocks and its application in geology and geophysics, *Geophys. Surv.,* **5,** 37–82.

Irving, E., Emslie, R. F. & Park, J. K., 1977. Palaeomagnetism of the Harp Lake complex and associated rocks, *Can. J. Earth Sci.,* **14,** 1187–1201.

Irving, E. & Hastie, J., 1975. *Catalogue of Palaeomagnetic Directions and Poles,* 2nd issue, Geomagnetic Series No. 3, Ottawa, Canada.

Jepsen, H. F., 1971. The Precambrian, Eocambrian and early Palaeozoic stratigraphy of the Jørgen Brønlund Fjord area, Peary Land, North Greenland, *Bull. Grønn. geol. Unders.,* **96,** 42 pp.

Jepsen, H. F. & Kalsbeek, F., 1979. Igneous rocks in the Proterozoic platform of eastern North Greenland, *Rapp. Grønn. geol. Unders.,* **88,** 11–14.

Jepsen, H. F., Kalsbeek, F. & Suthern, R. J., 1980. The Zig-Zag Dal Basalt Formation, North Greenland, *Rapp. Grønn. geol. Unders.,* **99,** 25–32.

Kalsbeek, F. & Jepsen, H. F., 1983. The Zig-Zag Dal Basalt of North Greenland – regional setting, field relations, petrography and chemical composition, unpublished manuscript.

Khan, M. A., 1962. The anisotropy of magnetic susceptibility of some igneous and metamorphic rocks, *J. geophys. Res.,* **67,** 2873–2885.

Larsen, O. & Graff-Petersen, P., 1980. Sr-isotropic studies and mineral composition of the Hagen Brae Member in the Proterozoic clastic sediments at Hagen Brae, eastern North Greenland, *Rapp. Grønn. geol. Unders.,* **99,** 111–118.

Marcussen, C., 1981. Continuation of the palaeomagnetic field work in eastern North Greenland, *Rapp. Grønn. geol. Unders.,* **106,** 95–98.

McElhinny, M. W., 1973. *Palaeomagnetism and Plate Tectonics,* Cambridge University Press, 358 pp.

Murthy, G. S., 1978. Palaeomagnetic results from the Nain anorthosite and their tectonic implications, *Can. J. Earth Sci.,* **15,** 516–525.

Palmer. H. C., Merz, B. A. & Hayatsu, A., 1977. The Sudbury dykes of the Grenville Front region: palaeomagnetism, petrochemistry, and K-Ar studies, *Can. J. Earth Sci.,* **16,** 1867–1887.

Patchett, P. J., Bylund, G. & Upton, B. G. J., 1978. Palaeomagnetism and the Grenville orogeny: new Rb-Sr ages from dolerites in Canada and Greenland, *Earth planet. Sci. Lett.,* **40,** 349–364.

Piper, J. D. A., 1976. Palaeomagnetism of marginal syenites and fractionated rocks of the Ilímaussaq intrusion, South Greenland, *Bull. geol. Soc. Denmark,* **25,** 89–97.

Piper, J. D. A., 1977a. Magnetic stratigraphy and magnetic-petrological properties of Precambrian Gardar lavas, South Greenland, *Earth planet. Sci. Lett.,* **34,** 247–263.

Piper, J. D. A., 1977b. Palaeomagnetism of the giant dykes of Tugtutôq and Narssaq Gabbro, Gardar Igneous Province, South Greenland, *Bull. geol. Soc. Denmark,* **26,** 85–94.

Piper, J. D. A. & Stearn, J. E. F., 1977. Palaeomagnetism of the dyke swarms of the Gardar Igneous Province, South Greenland, *Phys. Earth planet. Int.,* **14,** 345–358.

Scott, G. R., 1976. Palaeomagnetism of the Pioneer Shale (1300–1350 Ma) and associated high temperature TRM, *Eos, Trans. Am. geophys. Un.,* **57,** 902.

Stephenson, A. & de Sa, A., 1970. A simple method for the measurement of the temperature variation of initial magnetic susceptibility between 77 and 1000 K, *J. Phys.E:Sci. Instrum.,* **3,** 59–61.

Stupavsky, M. & Symons, D. T. A., 1978. Separation of magnetic components from AF step demagnetization data by least-squares computer methods, *J. geophys. Res.,* **83,** 4925–4932.

Thorning, L. & Abrahamsen, N., 1980. Palaeomagnetism of Permian multiple intrusion dykes in Bohuslän, SW Sweden, *Geophys. J. R. astr. Soc.,* **60,** 163–186.

Watson, G. S., 1956. Analysis of dispersion on a sphere, *Mon. Not. R. astr. Soc. Geophys. Suppl.,* 7, 153–159.

Watson, G. S. & Irving, E., 1957. Statistical methods in rock magnetism, *Mon. Not. R. astr. Soc. Geophys. Suppl.,* **7,** 289–300.

Wells, J. M. & Verhoogen, J., 1967. Late Palaeozoic palaeomagnetic poles and the opening of the Atlantic ocean, *J. geophys. Res.,* **72,** 1777–1781.

Wing-Fatt, L. & Stacey, F. D., 1966. Magnetic anisotropy of laboratory materials in which magma flow is simulated, *Pure appl. Geophys.,* **64,** 78–80.